

Glasslike character of molecular ordering in discotic lyomesophases

I. Drevensšek Olenik,¹ L. Spindler,² M. Čopič,¹ H. Sawade,³ D. Krüerke,³ and G. Heppke³

¹*Department of Physics, University of Ljubljana, Jadranska 19, SI-1000 Ljubljana, Slovenia
and J. Stefan Institute, Jamova 39, SI-1000 Ljubljana, Slovenia*

²*Faculty of Mechanical Engineering, University of Maribor, Smetanova 17, SI-2000 Maribor, Slovenia*

³*Technische Universität Berlin, Iwan-N.-Stranski-Institut, Strasse des 17. Juni 112, D-10623 Berlin, Germany*

(Received 25 July 2001; published 17 December 2001)

We studied dynamic light scattering from isotropic solutions of triphenylene derivative in dodecane at concentrations close to the isotropic-cholesteric phase transition that takes place at $c=25$ wt. % at room temperature. The correlation decay $g^{(2)}(t)$ reveals the presence of three dynamic modes, from which two appear in polarized (VV) and one in depolarized (VH) scattering. The VH mode, which is independent of the scattering wave vector q , exhibits an Arrhenius type temperature dependence and shows a strong deviation from the exponential relaxation associated with the stretching-exponent parameter $\beta_{VH} \sim 0.5$ for all the investigated concentrations. The VV modes both exhibit a quadratic dispersion of the inverse relaxation time $1/\tau$ on the scattering wave vector q . For concentrations $5 \text{ wt. \%} < c < 25 \text{ wt. \%}$ the temperature dependence of the fast VV mode obeys the Vogel-Fulcher-Tamman relation that is correlated with the nonexponential character of the relaxation. The corresponding stretching-exponent parameter β_{fast} decreases by increasing concentration and decreasing temperature. The slow VV mode, on the contrary, is always close to exponential behavior and shows an Arrhenius type temperature dependence, but it exhibits strong variations in relation with sample annealing and preparation procedures. The relaxation rates of all the modes strongly decrease with increasing triphenylene concentration. The observed dynamical properties suggests on the glasslike structure of large columnar aggregates formed in the pretransitional phase.

DOI: 10.1103/PhysRevE.65.011705

PACS number(s): 61.30.St, 81.16.Dn, 61.30.Eb

I. INTRODUCTION

Columnar liquid crystalline phases of disc-shaped molecules exhibit strongly anisotropic electronic transport properties that are related to unidirectional intermolecular coupling along the column axis. This feature makes columnar liquid crystals interesting candidates for applications in various kinds of optoelectronic devices such as, for example, photoconductive switches and organic light emitting diodes [1,2]. If the molecules forming columnar stacks are chiral and tilted with respect to column axis, ferroelectricity can also occur, which provides a possibility for bistable switching of the material parameters by a relatively low-magnitude external electric field [3]. One of the drawbacks in this respect is, however, that most of the pure discotic liquid crystals are highly viscous in their mesomorphic state and consequently a reasonably fast ferroelectric response can be achieved only at high temperatures just below the clearing point [4]. A possible solution of this problem is a solvation of the material in an appropriate solvent, which might be either polar or apolar [5–12]. This procedure usually brings two advantages: it reduces the viscosity and lowers the transition temperatures, so that room temperature ferroelectric columnar lyomesophases are achieved that might be in some cases competitive to the conventional ferroelectric SmC* phase.

If properly designed, the disk-shaped molecules in solution have a tendency to linearly self-assemble into columnar aggregates that grow in size by increasing concentration and/or decreasing temperature [13] (Fig. 1). The transition from isotropic to columnar nematic or cholesteric phase takes place when the average length of the columns becomes large enough to attain the Onsager's limit for phase transition

in the system of rodlike particles [14]. The average length and distribution of sizes of the columns play an important role also in determining the structural and viscoelastic properties of the mesophases and are hence crucial for the dynamic response of the material to external fields. At present there are, nevertheless, relatively few experimental data available on the process of formation of columnar aggregates in discotic lyomesomorphic systems and consequently relation between the self-assembling features and the properties of the mesophases is still far from being resolved.

We have recently reported on the phase diagram and switching characteristics of the lyomesophases observed in the mixture of chiral triphenylene derivative DLT 2 (Fig. 2) with dodecane [15,16]. At room temperature this mixture undergoes the isotropic to cholesteric (*I*-Ch) phase transition at concentration $c=25$ weight percent (wt. %) of DLT 2 in dodecane. The cholesteric phase is observed in the interval of $25 \text{ wt. \%} < c < 55 \text{ wt. \%}$. At even higher concentrations, prior to the crystallization, two soft columnar mesophases also appear.

For concentrations between 10 wt. % and 25 wt. %, a peculiar viscous isotropic state is observed that exhibits a strong flow induced birefringence and a large optical Kerr effect. These properties are, in our opinion, a manifestation of the pretransitional phenomena related to the cholesteric phase. In this paper, we report on the experimental investigation of the pretransitional phase by dynamic light scattering (DLS) technique. This method probes a dynamic response of the system in the interval of time scales from 10^{-8} s to 10^3 s. We found that the dynamic properties of the isotropic DLT 2/dodecane solution resemble a glasslike structure that is presumably related to an extensive intercolumnar

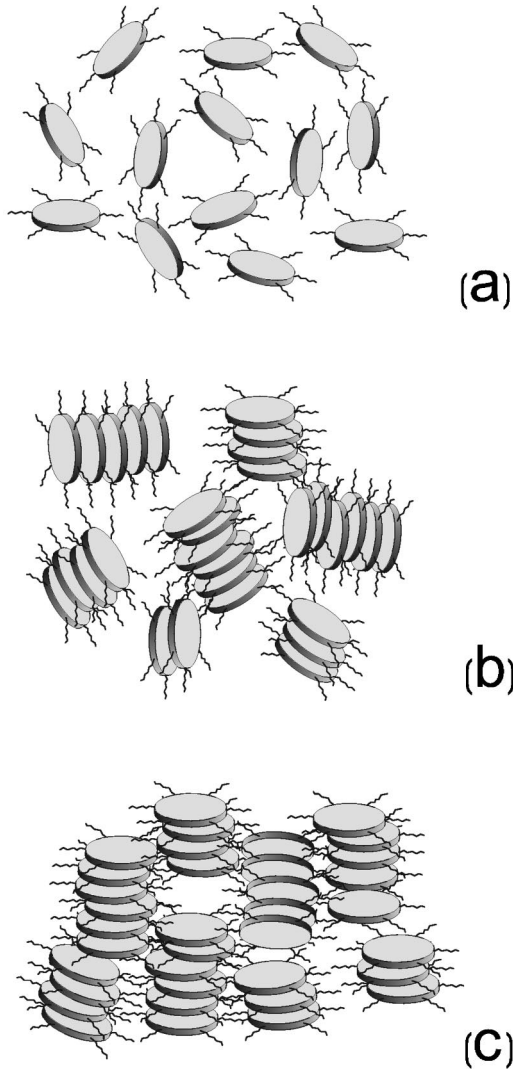


FIG. 1. Schematic representation of the presumed supramolecular assemblies formed at various concentrations: (a) nonaggregated isotropic phase, (b) columnar isotropic phase, (c) columnar nematic phase. The concentration increases from (a) to (c).

steric coupling. Similar features are supposed to determine also the dynamic properties of the lyomesogenic phases.

II. MATERIALS AND METHODS

The sample mixtures were prepared in the following way: a desired quantity of the DLT 2 and dodecane was mixed in

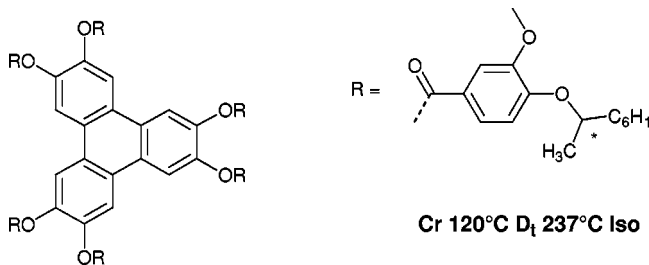


FIG. 2. Chemical structure and transition temperatures of the pure triphenylene derivative DLT 2 ($M=1898$ g/mol).

a closed glass capillary tube heated to 200 °C. After cooling the mixture to room temperature it was weighed again and the exact composition was calculated. The investigated mixtures had concentrations in the interval from 0.01 wt. % to 33 wt. % of DLT 2 in dodecane. The mesomorphic state of the samples was determined by polarization optical microscopy. The $c=33$ wt. % sample was in the cholesteric phase at room temperature and had a clearing point at about 373 K. All the other samples were isotropic in the range of the investigated temperatures. The capillary was put into the temperature controlled container filled with glycerine and mounted in the center of the goniometric stage. For some of the temperature dependence measurements the mixture was also introduced into a flat cell made from two glass substrates and mounted into the microscopic hot stage (Instec HS1-i). The glass plates were separated with 80 μm thick spacers and were sealed together with a two-component epoxy resin. The measurements were performed in the temperature range from 294 K to 394 K.

DLS measurements were performed using an ALV 5000 digital correlator and a He-Ne laser ($\lambda=632.8$ nm) as a light source. The normalized homodyne intensity autocorrelation function $g^{(2)}(t)=\langle I(0)I(t)\rangle/\langle I(t)\rangle^2$ was measured. Polarization of the incident laser beam was always perpendicular to the scattering plane (V polarization), while the polarization of the scattered light was selected to be either perpendicular (V polarization) or parallel (H polarization) to the scattering plane.

In the Gaussian approximation the normalized field correlation function of the scattered light $g^{(1)}(t)=\langle E(0)E(t)\rangle/\langle E(t)\rangle^2$ is related to $g^{(2)}(t)$ by the Siegert relation [17]

$$g^{(2)}(t)=1+\alpha|g^{(1)}(t)|^2, \quad (1)$$

where α is the spatial coherence factor that had a value of 1 in our detection setup using a single mode optical fiber. The field correlation function is associated with the dynamic structure factor of the material [18]

$$S(\vec{q},t)=\frac{1}{v^2}\int_v\int_v[\langle\varepsilon_{ij}(\vec{r},0)\varepsilon_{ij}(\vec{r}',t)\rangle - \langle\varepsilon_{ij}\rangle^2]e^{i\vec{q}\cdot(\vec{r}-\vec{r}')}d^3rd^3r', \quad (2)$$

which is in homodyne experiment related to $g^{(1)}(t)$ as

$$g^{(1)}(\vec{q},t)=S(\vec{q},t)/S(\vec{q},0), \quad (3)$$

where $\langle \rangle$ denotes time averaging, v the scattering volume and ε_{ij} with $i,j=V,H$ a projection of the optical dielectric tensor onto the polarizations of the incoming and the scattered beam, respectively. The magnitude of the scattering wave vector is given by $q=(4\pi n/\lambda)\sin(\theta/2)$ where n is the refractive index of the solution and θ the scattering angle selected by the position of the goniometric stage.

For dynamic response of a relaxational type $S(\vec{q},t)$ can be expressed as [17,19]

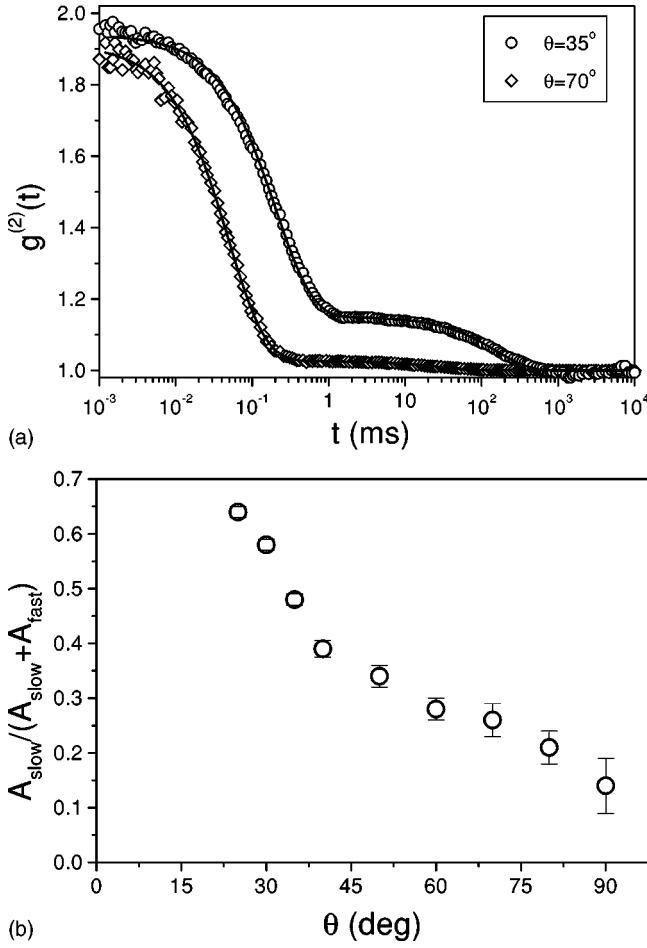


FIG. 3. (a) Autocorrelation functions of the VV scattered light measured in $c = 15$ wt. % solution at $T = 336$ K for two different scattering angles. Solid lines represent fits in accordance to Eqs. (1)–(4). (b) Typical angular dependence of the relative amplitude of the slow mode.

$$S(\vec{q}, t) = \sum_l A_l e^{(-t/\tau_l)\beta_l}, \quad (4)$$

where A_l is the amplitude and τ_l the relaxation time of the l th dynamic mode. The Kohlrausch-Williams-Watts (KWW) parameter β_l , which is in the range of $0 < \beta_l < 1$, characterizes a deviation of the mode from an exponential decay. Its value decreases by increasing polydispersity of the intrinsic response times of the system. Very broad distributions of dynamic response times are typical for glass forming liquids and for gel-forming solutions near the sol-gel transition temperature [19–23].

If the relaxation time τ_l of the specific mode depends on the scattering wave vector q then its apparent diffusion coefficient $D_l = 1/(\tau_l q^2)$ is commonly calculated. It is related to a characteristic spatial correlation length ξ_l of the system by [17]

$$D_l = kT / (6\pi\eta\xi_l), \quad (5)$$

where η is the viscosity and T the temperature of the solution.

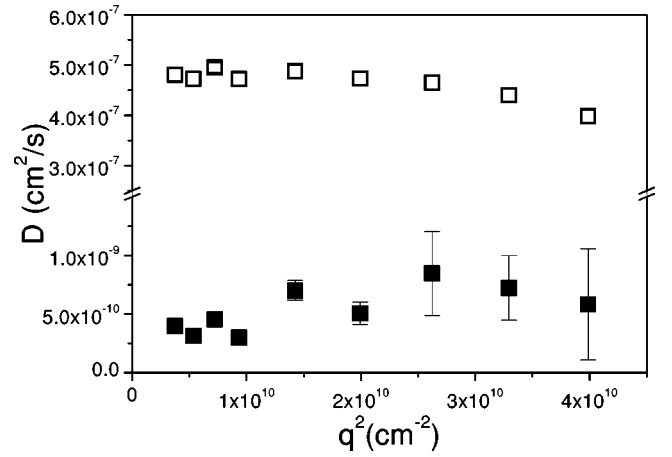


FIG. 4. Angular dependence of the diffusion coefficient of the fast mode (open symbols) and the slow mode (solid symbols) measured at $T = 336$ K in $c = 15$ wt. % sample.

The average intensity of the scattered light $\langle I(\vec{q}, t) \rangle$ in a selected direction is determined by the static structure factor $S(\vec{q}, 0)$ [Eq. (2)]. For dilute solutions of scattering centres of a size much smaller than optical wavelength λ the corresponding differential cross section is given by the Rayleigh formula [24]

$$\sigma(\vec{q}) = \pi^2 V^2 \langle \Delta \varepsilon_{ij}^2 \rangle f(\vec{q}) / \lambda^4, \quad (6)$$

where V is the apparent hydrodynamic volume of a single scattering object, $\Delta \varepsilon_{ij}$ a difference between the dielectric tensor of the scattering substance and the solution, and $f(\vec{q})$ a factor depending on selected scattering direction and polarizations. Modifications of $\langle I(\vec{q}, t) \rangle$ at known concentration, therefore, give evidence on the structural transformations of the dissolved material.

III. RESULTS

A. Angular dependence

The $g^{(2)}(t)$ autocorrelation functions measured in the VV scattering regime show two clearly separated dynamic modes, which we denote as the fast and the slow mode [Fig. 3(a)]. The corresponding values of the relaxation times τ_{slow} and τ_{fast} differ by about three orders of magnitude. At low temperatures the stretching exponent (KWW) parameter β_{fast} for concentrated samples is significantly below 1, while $\beta_{slow} \sim 1$. These parameters are practically independent of the scattering angle θ . The relative amplitude of the slow mode $A_{slow} / (A_{slow} + A_{fast})$ strongly decreases with increasing the scattering angle θ [Fig. 3(b)]. Both VV modes exhibit a nearly quadratic dispersion of the inverse relaxation time $1/\tau$ on the scattering wave vector q . The associated diffusion coefficients as a function of the scattering wave vector are given in Fig. 4. Only some slight deviations from a constant value can be noted.

The DLS response in the VH scattering regime shows solely one dynamic mode with an apparent relaxation time τ_{VH} in the intermediate region between τ_{fast} and τ_{slow} of the

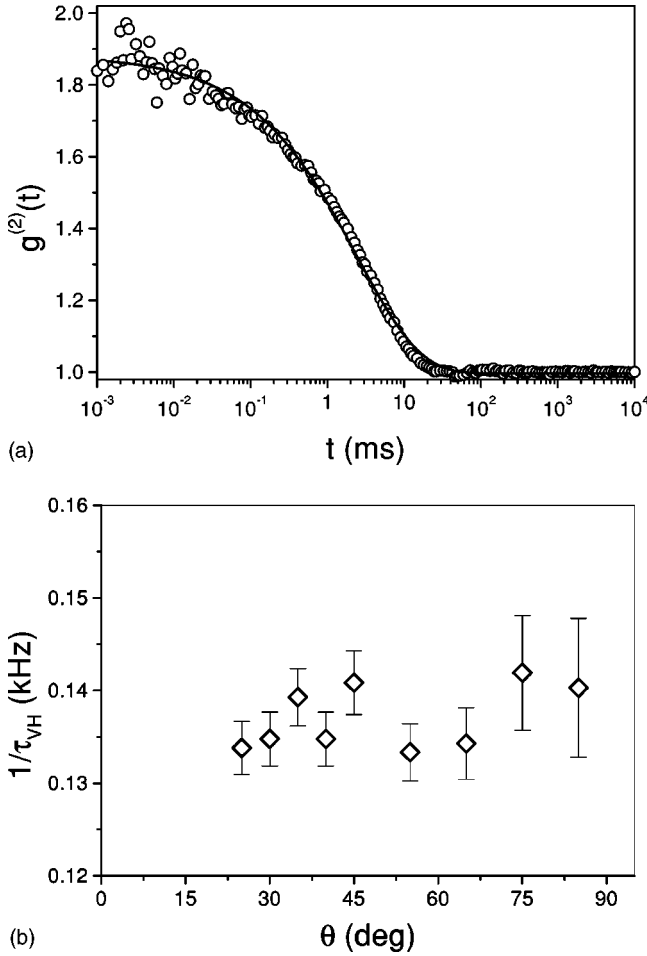


FIG. 5. (a) Autocorrelation function of the VH scattered light measured in $c = 15$ wt. % solution at $\theta = 35^\circ$ and $T = 296$ K. Solid line represents fit in accordance to Eqs. (1)–(4). (b) Angular dependence of the relaxation rate of the slow mode.

VV modes [Fig. 5(a)]. The mode is strongly nonexponential with the stretching exponent parameter $\beta_{VH} \sim 0.5$. The intensity of the VH scattered light and also the value of β_{VH} slightly increase with decreasing scattering angle θ , while τ_{VH} does not exhibit any significant angular dependence [Fig. 5(b)].

B. Temperature dependence

The average intensity of the VV scattered light is temperature independent (Fig. 6). The dynamic properties of the VV modes, on the contrary, exhibit pronounced temperature and concentration induced variations. For large concentrations and low temperatures the VV fast mode strongly deviates from a single exponential relaxation, while at higher temperatures or lower concentrations it shows an approximately exponential decay. Figure 7 shows the results for $c = 17.5$ wt. % (a) and $c = 1$ wt. % (b). For 17.5 wt. % sample the value of stretching exponent parameter β_{fast} is nearly constant in the temperature region corresponding to an approximately exponential relaxation, while the nonexponential relaxation is related to the values of β_{fast} significantly below 0.9. It can also be noted that for region with

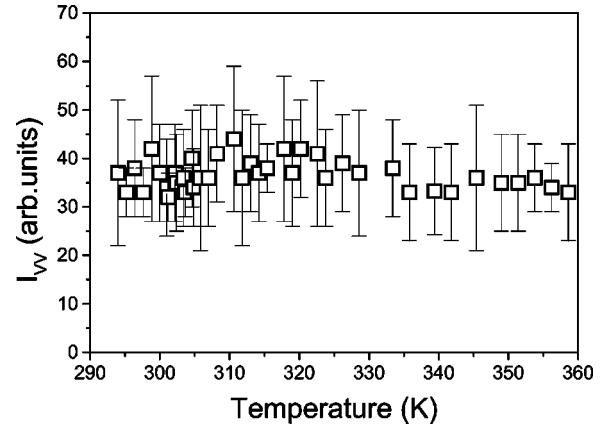


FIG. 6. Temperature dependence of the average intensity of the VV scattered light measured at $\theta = 50^\circ$ in $c = 17.5$ wt. % sample.

$\beta_{fast}(T) \sim \text{const}$ the inverse relaxation time $1/\tau_{fast}$ exhibits an Arrhenius type temperature dependence

$$1/\tau_{fast} = (1/\tau_0)e^{-W_a/kT}, \quad (7)$$

where W_a is the activation energy, which is of the order of 0.5 eV. In the region with strongly varying $\beta_{fast}(T)$ the behavior of $1/\tau_{fast}(T)$ is no longer in accordance with the Arrhenius law [Fig. 7(a)]. A fit can be obtained by using the Vogel-Fulcher-Tamman (VFT) relation [22,25]

$$1/\tau_{fast} = (1/\tau_{VFT})e^{-B/(T-T_0)}, \quad (8)$$

where T_0 is an apparent freezing temperature of the mode. In accordance with this feature a characteristic “transition” temperature T_A is defined as the temperature at which the Arrhenius behavior converts to the VFT behavior [26]. In $c = 1$ wt. % sample [Fig. 7(b)], on the contrary, the value of β_{fast} is always nearly the same and the Arrhenius type temperature dependence of $1/\tau_{fast}$ is detected for all the investigated temperatures.

The inverse relaxation time of the VV slow mode $1/\tau_{slow}$ strongly increases with increasing temperature. It exhibits the Arrhenius type temperature behavior for all the investigated concentrations (Fig. 8). The corresponding activation energy $W_{a,slow}$ is of a range of 1 eV and decreases with increasing concentration (Fig. 11). For this mode it is specific that its relative amplitude $A_{slow}/(A_{slow} + A_{fast})$ at selected scattering angle θ strongly depends on the sample preparation procedure and usually also decreases by sample aging.

The average intensity of the depolarized (VH) scattered light in the isotropic phase is in general at least one order of magnitude lower than the intensity of the VV scattered light. It decreases continuously by increasing temperature (Fig. 9). The value of the stretching-exponent parameter $\beta_{VH} \sim 0.5$ for the VH mode is practically independent of temperature and concentration for all the concentrations at which the mode was still detectable ($c > 1$ wt. %) (Fig. 10). The apparent relaxation time τ_{VH} always shows the Arrhenius type temperature dependence with activation energy $W_{a,VH}$ in the range of 1 eV (Fig. 10, Fig. 11).

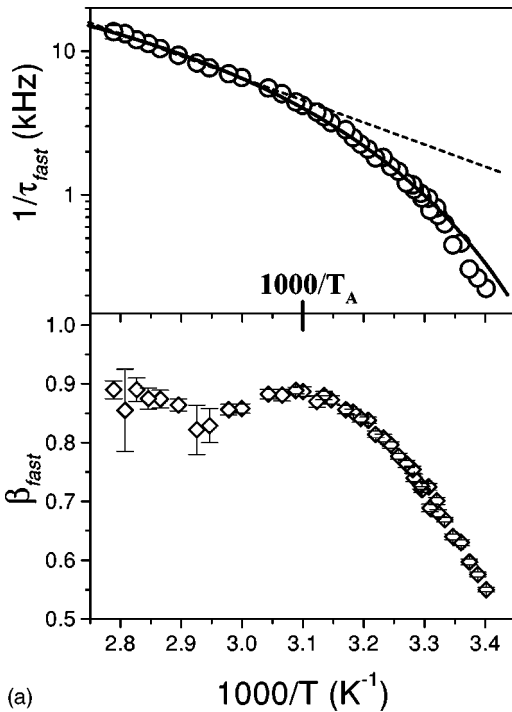


FIG. 7. Temperature dependence of the inverse relaxation time and the stretching-exponent parameter of the fast VV mode measured at $\theta=50^\circ$ in (a) $c=17.5$ wt. % sample and (b) $c=1$ wt. % sample. Dashed lines are fits to Eq. (7) (performed in the interval $T>T_A$), while solid line is a fit to Eq. (8). In (a) the transition from Arrhenius to VFT dependence takes place at $T=T_A$.

C. Concentration dependence

Figure 11 shows the concentration dependence of the activation energy W_a calculated in accordance with Eq. (7) for all the three modes. The values for the VV fast mode in

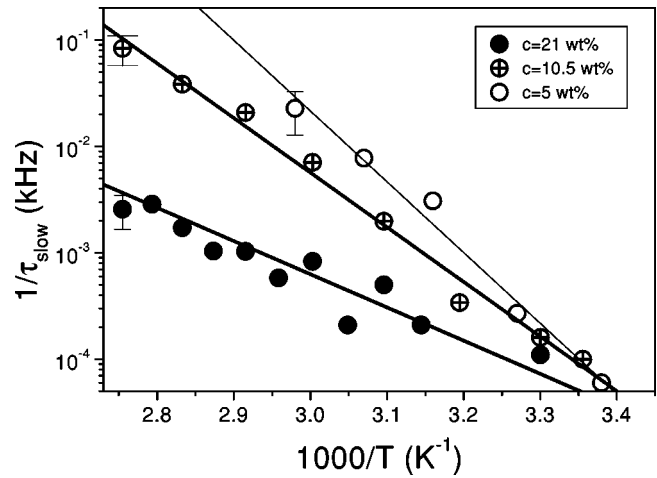


FIG. 8. Temperature dependence of the inverse relaxation time of the VV slow mode measured at $\theta=50^\circ$ for various concentrations. Solid lines are fits to Eq. (7).

concentrated samples were deduced from a fit of the experimental data within the limited temperature region $T>T_A$ that corresponds to the Arrhenius behavior. Activation energies of both VV modes decrease by increasing concentration with the values for the fast mode being about three times lower than the values for the slow mode. The results for the VH mode, conversely, do not show any systematic changes.

The concentration dependence of the temperature T_A related to transformation from the Arrhenius to the VFT law for the VV fast mode is given in Fig. 12. For concentrations $c<2.5$ wt. % the transition presumably takes place below the temperatures attainable by our experimental setup. The value of T_A monotonously increases with increasing concentration. The corresponding “freezing” temperature T_0 [Eq. (8)] is about 70 K below T_A .

At fixed temperature the inverse relaxation time $1/\tau$ of all the modes decreases by increasing concentration (Fig. 13). This variation is most pronounced for the HV mode, which slows down for more than two orders of magnitude in the interval of 1 wt. % $<c<21$ wt. %. The relatively large experimental errors of the data for the VV slow mode are the

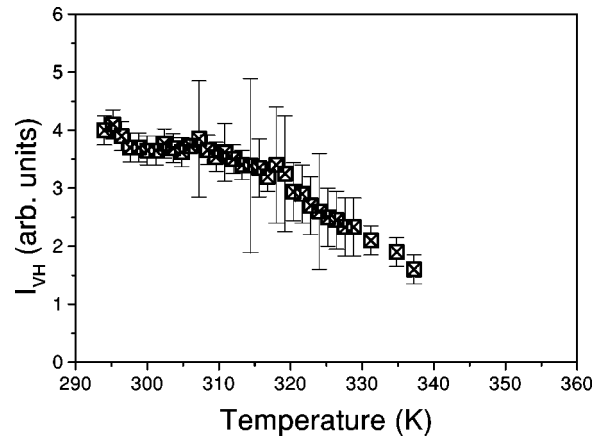


FIG. 9. Temperature dependence of the average intensity of the VH scattered light measured at $\theta=50^\circ$ in $c=17.5$ wt. % sample.

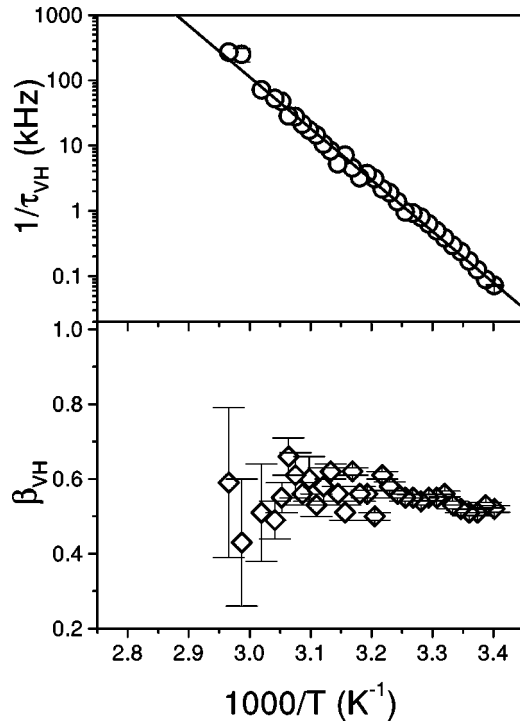


FIG. 10. Temperature dependence of the inverse relaxation time and the stretching-exponent parameter of the VH mode measured at $\theta=50^\circ$ in $c=17.5$ wt. % sample.

consequence of the low amplitude and long relaxation time of this mode at room temperature, while the nonmonotonous behavior is probably due to different history of various samples.

IV. DISCUSSION

A. Fast VV mode

The polarized VV dynamic light scattering probes primarily the translational diffusion of the aggregates [17]. Theoretical models of the linear self-assembling process predict an about exponential distribution of aggregate sizes, with the average length of the columns that monotonously increases

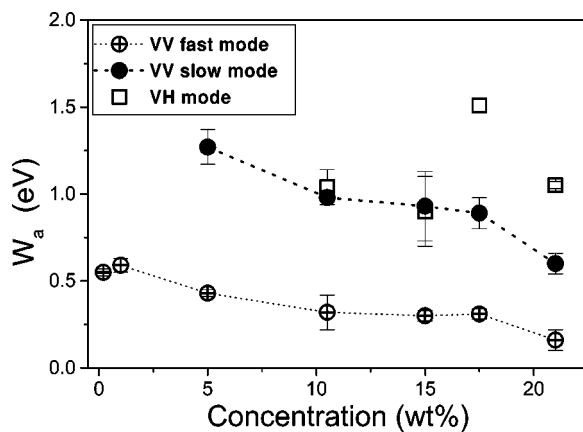


FIG. 11. The activation energy of various modes as a function of concentration. The dotted lines are guides to the eye.

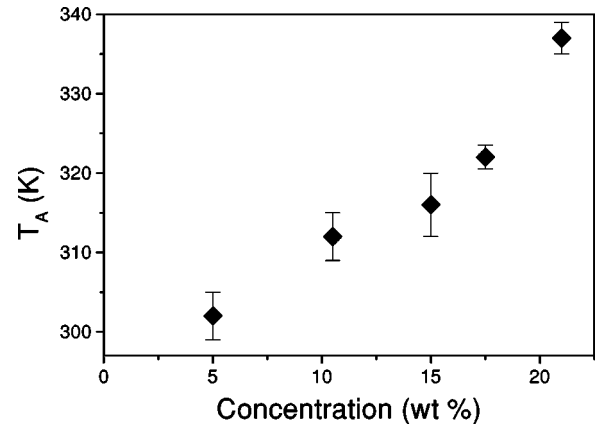


FIG. 12. Concentration dependence of the temperature at which the VV fast mode transforms from the Arrhenius to the VFT behavior.

by decreasing temperature and increasing concentration [13,26]. Such a polydisperse distribution of sizes was recently reported in relation with the proton NMR performed in isotropic phase of aqueous solution of a triphenylene derivative [27,28]. A polydisperse distribution of columnar lengths could also explain a large distribution of DLS response times of the VV fast mode observed in our experiments. If considering the columns as noninteracting rigid rods, the translational diffusion coefficient of a stack of m disks is given by Eq. (5) [29]

$$D_m = [kT \ln(L_m/b)] / 3\pi\eta L_m, \quad (9)$$

where b is an apparent diameter of a single disk, $L_m = md$ is the column length, and d the interstacking distance. In case

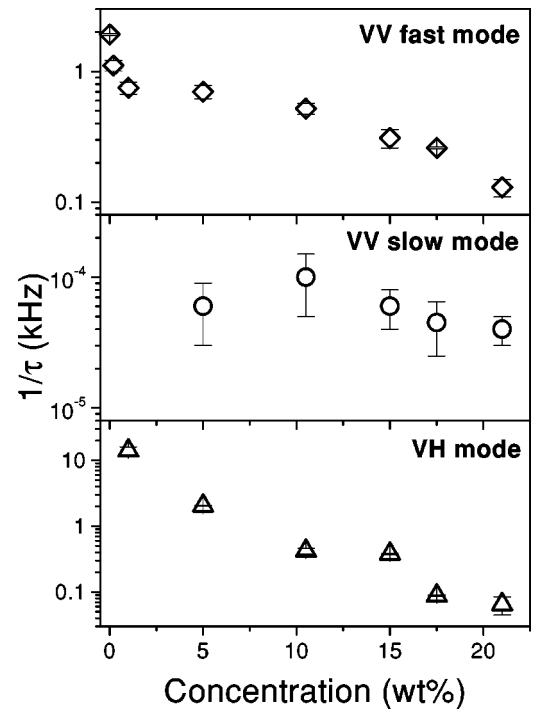


FIG. 13. Concentration dependence of the inverse relaxation time of various modes measured at $\theta=50^\circ$ and $T=295$ K.

of strong association the average number of the disks in a single stack $\langle m \rangle$ is much larger than 1 and consequently a broad distribution of corresponding relaxation times is expected.

In our experimental results there are, however, many aspects that do not agree with the above given simple explanation for the nonexponential relaxation. At first, a change of the average column length should be accompanied also with the modification of the average intensity of the scattered light $\langle I_{VV}(\vec{q}, t) \rangle$. For an exponential distribution of column sizes with $M_0 \gg \langle m \rangle \gg 1$ it follows from Eq. (6) that

$$\langle I_{VV}(\vec{q}, t) \rangle \propto \sum_{m=1}^{M_0} N_m V_m^2 \approx \langle m \rangle M_0 V_0^2, \quad (10)$$

where M_0 is a total number of the disks, N_m the volume density of the columns formed from m disks and $V_m = m V_0$ and V_0 are apparent hydrodynamic volumes of a single column and a single disk, respectively. Bearing in mind Eq. (10) and, for example, the temperature dependence of the inverse relaxation time $1/\tau_{fast}$ as shown in Fig. 7(a), the intensity of the scattered light should decrease by increasing temperature in accordance with decreasing $\langle m \rangle$ until a complete dissociation of the columns presumably take place at $T = T_A$. Contrary to this, we have observed no variation of the $\langle I_{VV} \rangle$ in the whole investigated temperature range (Fig. 6). This suggests that the observed changes of the dynamical properties of the VV modes are related to the modifications of the effective viscosity of the medium and not to the modifications of its aggregation structure.

The room temperature (297 K) viscosity of the DLT 2/dodecane mixture in pre-translational phase strongly increases with increasing concentration. Measurements with the shear viscosimeter (Brookfield DV-II+) have shown that in the $c = 0.04$ wt. % sample its value ($\eta = 1.4$ cP) is still similar to the viscosity of the pure dodecane ($\eta_s = 1.35$ cP), but already in the $c = 0.2$ wt. % solution it increases to 1.7 cP which suggests on substantial intercolumnar interactions. The above formula for free particle diffusion [Eq. (9)] is hence expected to be adequate only for the most diluted measured solution of $c = 0.04$ wt. %. At this concentration the mode exhibits an approximately exponential relaxation with $D_{fast} = (1.5 \pm 0.4) \times 10^{-7}$ cm²/s corresponding to $\xi_{fast} = 11 \pm 2$ nm [Eq. (5)].

As a next step we calculate the size of the aggregates associated with above value for ξ_{fast} . According to the molecular modeling the diameter of a completely relaxed DLT 2 molecule is $b_{max} \sim 4$ nm, while the rigid triphenylene core has a diameter $b_{core} \sim 1.2$ nm [14,30]. The apparent hydrodynamic diameter of the molecule is expected to be somewhere in between these two limiting values. Furthermore, the interstacking distance in a pure discotic compound of a triphenylene derivative similar to DLT 2 was found to be 0.36 nm [30]. By inserting an average diameter $b = 2.6$ nm and $d = 0.36$ nm into Eq. (9) the value $L = 74 \pm 13$ nm is achieved for the column length corresponding to $\langle m \rangle = 205 \pm 50$. The columns formed in the DLT 2/dodecane system at $c = 0.04$ wt. % are hence already very long. Be-

sides this, due to nearly exponential relaxation of the fast mode, their size distribution is quite monodisperse. The free volume of a single column at this concentration is $v_f = (\langle m \rangle M) / (c \rho N_A) = 2.1 \times 10^{-21}$ m³ which corresponds to $5L^3$. This result indicates that we are close to the limit of the dilute solution regime and hence intercolumnar interactions are expected to become important at higher concentrations. The transformation from dilute to semidilute regime should appear at $v_f \sim L^3$, i.e., at $c \sim 0.2$ wt. %. Accordingly to this, by increasing concentration, the translational diffusion rate $1/\tau_{VV}$ is at first reduced for about a factor of two (Fig. 13), in agreement with the properties of semidilute solutions of rigid rods [29].

If we assume that the average column length remains the same ($L = 74$ nm) also at higher concentrations, then in the $c \sim 5$ wt. % sample the free volume v_f will reduce to bL^2 , i.e., to the excluded volume of a single column [29]. At this concentration hence the solution converts from semidilute to concentrated. We propose that a pronounced steric linking and entanglement of the congested columns via their branched side chains starts to take place at about this concentration and for $c > 5$ wt. % further slows down the fast mode (Fig. 13). It also induces strong coupling between the translational and rotational degrees of freedom that results in a glasslike dynamic response of the system, i.e., in a pronounced nonexponential relaxation and the non-Arrhenius temperature dependence of the apparent relaxation time.

B. Slow VV mode

The origin of the VV slow mode is, on the other hand, much more unclear. One of the puzzling features is that its properties are sensitive to the sample preparation and history and hence the reproducibility of the results is not very good. A mode with similar properties was detected in some polymeric gel forming systems and was attributed to the complex network relaxation [31,32]. An ultraslow mode is often found also in solutions of star polymers and in many glass-forming liquids and is generally related to the strong excess scattering at low scattering angles [21,33], which is the feature that was observed also in our experiments [Fig. 3(b)].

C. VH mode

The depolarized VH scattering is related to rotational diffusion of the aggregates. Contrary to the VV fast mode, the VH mode exhibits a remarkably broad distribution of relaxation times at all the temperatures and concentrations at which we were able to detect it. For the lowest analyzed concentration $c = 1$ wt. % the observed value of the inverse relaxation time ($1/\tau_{VH}$) = 15 kHz is already about ten times below the value $1/\tau = [18kT \ln(L/b)] / \pi \eta L^3$ expected for a free rotational diffusion of the rigid rods of $L = 74$ nm [29]. This is because in the semidilute regime the rotation of each column is severely restricted by the presence of other columns and consequently it becomes slower. These restrictions cause local short-range orientational ordering of the columns that represents a formation of transient nematiclike clusters in the isotropic phase. From this point of view the VH mode of the DLT 2/dodecane system is analogous to the pretransi-

tional orientational fluctuations detected in the vicinity of the nematic-isotropic phase transition in thermotropic liquid crystals [34,35].

The observed decrease of the VH scattering intensity with increasing temperature (Fig. 9) is attributed to the decrease of the local orientational order parameter of the clusters, while the prominent nonexponential nature of the VH mode suggests on strongly heterogeneous environments related to different clusters. This heterogeneity should remain also in the corresponding ordered state. In agreement with this assumption we have indeed observed an orientational dynamic mode with a similarly broad distribution of relaxation times ($\beta \sim 0.5$) in the $c = 33$ wt. % sample that was in the cholesteric phase. The cholesteric phase, therefore, corresponds to a pretransitional state of an orientationally ordered glass.

V. CONCLUSIONS

In semidilute concentration region the DLT 2/dodecane system resembles dynamic properties of solutions of stiff-chain polymers. This similarity originates from a relatively monodisperse size distribution of the self-assembled columnar stacks which are formed already in dilute isotropic phase and appear to be quite stable. The source of strong associative forces between amphiphilic triphenylene-based molecules in alkanes is not yet fully clarified. The association is very probably governed by the π - π interactions between the triphenylene cores [36], but the role of aromatic sidechains immersed in the alkane surrounding might also be quite important and still have to be resolved.

In concentrated solution intercolumnar steric “connections” are formed by overlapping of the molecular sidechains and lead to the fragile glasslike dynamic response of the system. The interconnected glassy structure seems to be an inherent property of the branched-type discotic mesogens and is very probably also a reason for the extraordinary slow response characteristic for the liquid crystalline state of pure compounds. This is also in agreement with the fact that glass transition can be detected in some discotic materials [37,38].

The presence of long columnar aggregates together with their extensive orientational coupling explains also a strong flow induced birefringence observed in the pretransitional phase of the DLT 2/dodecane solution. The flow is connected with the shear stress that acts as an aligning field for the columns, leading to their reorientation along the direction of the flow. This effect is expected to take place on the same time scale as the relaxation of the VH mode observed in our DLS measurements, i.e., in the range of several milliseconds. The corresponding birefringence may be additionally enhanced also by unidirectional π - π interaction between the adjacent DLT 2 molecules within the stacks. This mechanism, which can lead to a considerable increase of the optical susceptibility of a single column, is not yet verified and consequently represents an attractive subject for further investigations.

ACKNOWLEDGMENT

This work was supported by the EU network SILC (Contract No. ERB FMRXCT 980209).

-
- [1] For a recent review see for instance: S. Chandrasekhar, and S. Krishna Prasad, *Contemp. Phys.* **40**, 237 (1999).
- [2] N. Boden, and B. Movaghar, in *Handbook of Liquid Crystals*, edited by D. Demus, J. Goodby, G.W. Gray, H.-W. Spiess, and V. Vill (Wiley-VCH, New York, 1998), Vol. 2B, pp. 781–796.
- [3] H. Bock and W. Helfrich, *Liq. Cryst.* **12**, 697 (1992).
- [4] G. Heppke, D. Krüerke, M. Müller, and H. Bock, *Ferroelectrics* **179**, 203 (1996).
- [5] N. Boden, R.J. Bushby, and C. Hardy, *J. Phys. (Paris)* **46**, L-325 (1985).
- [6] N. Boden, R.J. Bushby, C. Hardy, and F. Sixl, *Chem. Phys. Lett.* **123**, 359 (1986).
- [7] B. Kohne, K. Praefcke, T. Derz, H. Hoffmann, and B. Schwander, *Chimia* **40**, 171 (1986).
- [8] N. Usol'tseva, K. Praefcke, D. Singer, and B. Gündogan, *Liq. Cryst.* **16**, 601 (1994).
- [9] N. Usol'tseva, K. Praefcke, D. Singer, and B. Gündogan, *Liq. Cryst.* **16**, 617 (1994).
- [10] N. Usol'tseva, G. Hauck, H.D. Koswig, K. Praefcke, and B. Heinrich, *Liq. Cryst.* **20**, 731 (1996).
- [11] A.R.A. Palmans, J.A.J.M. Vekemans, E.E. Havinga, and E.W. Meijer, *Angew. Chem. Int. Ed. Engl.* **36**, 2648 (1997).
- [12] A.R.A. Palmans, J.A.J.M. Vekemans, R.A. Hikmet, H. Fischer, and E.W. Meijer, *Adv. Mater.* **10**, 873 (1998).
- [13] N. Boden, R.J. Bushby, L. Ferris, C. Hardy, and F. Sixl, *Liq. Cryst.* **1**, 109 (1986).
- [14] M.P. Taylor, and J. Herzfeld, *J. Phys.: Condens. Matter* **5**, 2651 (1993).
- [15] D. Krüerke, P. Rudquist, S.T. Lagerwall, H. Sawade, and G. Heppke, *Ferroelectrics* **243**, 207 (2000).
- [16] G. Heppke, D. Krüerke, C. Löhning, D. Löttsch, D. Moro, M. Müller, and H. Sawade, *J. Mater. Chem.* **10**, 2657 (2000).
- [17] K.S. Schmitz, *An Introduction to Dynamic Light Scattering by Macromolecules* (Academic Press, San Diego, 1990).
- [18] B.J. Berne and R. Pecora, *Dynamic Light Scattering* (Wiley, New York, 1976).
- [19] G. Williams, *J. Non-Cryst. Solids* **131**, 1 (1991).
- [20] G. Meier, B. Gerharz, D. Boese, and E.W. Fischer, *J. Chem. Phys.* **94**, 3050 (1991).
- [21] R. Böhmer, K.L. Ngai, C.A. Angell, and D.J. Plazek, *J. Chem. Phys.* **99**, 4201 (1993).
- [22] E.W. Fischer, *Physica A* **201**, 183 (1993).
- [23] S. Maity, and H.B. Bohidar, *Phys. Rev. E* **58**, 729 (1998).
- [24] A. Ishimaru, *Wave Propagation and Scattering in Random Media* (Academic Press, New York, 1978) Vol. 1.
- [25] M. Ediger, C.A. Angell, and R. Nagel, *J. Phys. Chem.* **100**, 13 200 (1996).
- [26] M. Placidi, and S. Cannistraro, *Chem. Phys. Lett.* **310**, 130 (1999).
- [27] M.E. Cates, and S.J. Candau, *J. Phys.: Condens. Matter* **2**, 6869 (1990).

- [28] R. Hughes, A. Smith, R. Bushby, B. Movaghar, and N. Boden, *Mol. Cryst. Liq. Cryst.* **332**, 547 (1999).
- [29] M. Doi and S.F. Edwards, *The Theory of Polymer Dynamics* (Clarendon Press, Oxford, 1988).
- [30] We have calculated the diameter using the Dreiding model.
- [31] M.T. Allen, S. Diele, K.D.M. Harris, T. Hegmann, B.M. Karimuki, D. Lose, J.A. Preece, and C. Tschierske, *J. Mater. Chem.* **11**, 302 (2001).
- [32] M.C. Blanco, D. Leisner, C. Vazquez, and M.A. Lopez-Quintela, *Langmuir* **16**, 8585 (2000).
- [33] J. Stellbrink, J. Allgaier, and D. Richter, *Phys. Rev. E* **56**, R3772 (1997).
- [34] T.W. Stinson, and J.D. Litster, *Phys. Rev. Lett.* **25**, 503 (1970).
- [35] T.W. Stinson, and J.D. Litster, *Phys. Rev. Lett.* **30**, 688 (1973).
- [36] C.A. Hunter and J.K.M. Sanders, *J. Am. Chem. Soc.* **112**, 5525 (1990).
- [37] H. Groothues, F. Kremer, D.M. Collard, and C.P. Lillya, *Liq. Cryst.* **18**, 117 (1995).
- [38] B. Glösen, A. Kettner, J. Kopitzke, and J.H. Wendorff, *J. Non-Cryst. Solids* **24**, 113 (1998).